On the Calculation of Length Scales for Turbulent Heat Transfer Correlation

Michael J. Barrett
Asst. Professor
Mem. ASME
Valparaiso University,
Mechanical Engineering Department,
Valparaiso, IN 46383
e-mail: Michael.Barrett@valpo.edu

D. Keith Hollingsworth
Assoc. Professor
Mem. ASME
University of Houston,
Department of Mechanical Engineering,
Houston, TX 77204
e-mail: Hollingsworth@uh.edu

Turbulence length scale calculation methods were critically reviewed for their usefulness in boundary layer heat transfer correlations. Using the variance of the streamwise velocity and the dissipation spectrum, a rigorous method for calculating an energy-based integral scale was introduced. A principal advantage of the new method is the capability to calculate length scales in a low-Reynolds-number turbulent boundary layer. The method was validated with data from grid-generated, free-shear-layer, and wall-bounded turbulence. Length scales were calculated in turbulent boundary layers with momentum thickness Reynolds numbers from 400 to 2100 and in flows with turbulent Reynolds numbers as low as 90. [DOI: 10.1115/1.1391277]

Keywords: Heat Transfer, Turbulence

Introduction

The study of the effects of elevated free-stream turbulence on boundary layer heat transfer requires that the turbulence in the free-stream and in the boundary layer be adequately characterized. When attempting to describe a turbulent flow, a minimal set of descriptors to characterize the turbulence must include a velocity and a length scale (or parameters that yield the equivalent dimensional information). In many cases these two scales alone are inadequate; however, any attempt that does not include at least these two scales is incomplete.

A review of the literature reveals a plenitude of length scale definitions. Restricting our survey to heat transfer in turbulent boundary layers, we still find more than ten different length scales in use. In some instances, the interpretation of two scales is similar but distinct calculation methods distinguish one scale from another. In this paper we critically examine five length scales commonly used in turbulent boundary layer heat transfer correlations. We then introduce a rigorous method for calculating an energy-based scale; advantages and disadvantages of the new calculation method are discussed. Experimental data is used to clarify the guidelines and performance traits for the new method. Based on the versatility of the new calculation method, the consistent behavior and physical significance of the resulting scale, and the detail to which the calculation is defined, the method is proposed as a standard for future correlative works.

Review of Existing Scale Definitions

The five scales chosen for review are all integral scales. In that sense, the scales are related to the largest eddies or the width of a shear flow [1]. The first three scales are closely related to the Eulerian integral scale, Λ_f, which, when Taylor's hypothesis holds, is given by Hinze [2] as

$$\Lambda_f = UT_{11}, \tag{1}$$

where U is the time-mean Eulerian velocity in the principal flow direction and T_{11} is the Eulerian integral time scale. The time scale, T_{11}, is found by integrating the Eulerian autocorrelation coefficient,

$$T_{11} = \int_0^\infty R_{11} dt. \tag{2}$$

This length scale, Λ_f, may be interpreted as a measure of the longest correlation distance between the velocities at two points in the flow field [2].

The first scale for review is frequently used in the gas turbine literature and is given by

$$\Lambda_I = U \int_0^\infty R_{11,\ \text{measured}}\ dt. \tag{3}$$

Young et al. [3], Van Fossen et al. [4], Camp and Shin [5], and Moss and Oldfield [6] are just a few of the authors that use this scale. (Additional studies are listed in Table 1.) Authors often terminate the correlation coefficient integration at the first zero crossing.

The next two scales are based on von Karman's turbulence spectrum [2],

$$UE_1\{f\}/(\Lambda_f u'^2) = 4[1 + (8\pi f \Lambda_f/3U)^2]^{-5/6}, \tag{4}$$

where f is frequency and $E_1\{f\}$ is the power spectral density of the streamwise fluctuating component, u'. The term $E_1\{f\}$ is also called the one-dimensional energy spectrum. The second scale, Λ_{II}, is calculated by curve fitting a measured energy spectrum to Eq. (4). Hollingsworth and Bourgogne [7] and Maniam and Hollingsworth [8] determine length scales by varying Λ_{II} until a best fit to a measured spectrum is found. The third scale, Λ_{III}, is found by extrapolating a measured spectrum to its zero frequency value and applying Eq. (4) at f equals zero,

$$\Lambda_{III} = UE_1\{0\}/4u'^2. \tag{5}$$

Authors that use this scale include Thole et al. [9] and Johnson and Johnston [10]. The Λ_{III} scale relies heavily on low frequency (low wave number) information.

The final two scales for review are termed "energy scales" because the definitions are related to the dissipation of turbulent kinetic energy, ϵ. In each case, there exists an underlying tie to the inviscid decay relation,

$$\epsilon \sim (u'^2)^{3/2}/L. \tag{6}$$

Each scale may be interpreted as an average length scale for the energy-containing eddies. The first of these two scales was given by Simonich and Bradshaw [11] as

Contributed by the Heat Transfer Division for publication in the JOURNAL OF HEAT TRANSFER. Manuscript received by the Heat Transfer Division January 26, 2000; revision received December 18, 2000. Associate Editor: R. L. Mahajan.

Table 1 Length scales used in example studies

Study	Λ_I	Λ_{II}	Λ_{III}	L_I	L_{II}
Simonich and Bradshaw [11]				•	
Blair [16]				•	
Hancock and Bradshaw [19]				•	
Castro [18]				•	
Hancock and Bradshaw [17]				•	
Johnson and Johnston [10]			•	•	
Ames and Moffat [12]	•				•
Sahm and Moffat [20]	•				•
Young, et al. [3]	•				
Thole, et al. [9]	•		•	•	
Hollingsworth and Bourgogne [7]		•			
Camp and Shin [5]	•				
Ames and Plesniak [21]	•				•
Thole and Bogard [22]	•		•	•	
Van Fossen, et al. [4]	•				
Thole and Bogard [23]	•		•	•	
Moss and Oldfield [6]	•				
Ames [24]	•				•
Bott and Bradshaw [25]				•	
Maniam and Hollingsworth [8]		•			

$$L_I = -(u'^2)^{3/2}/U \frac{d(u'^2)}{dx}. \quad (7)$$

The streamwise decay of u'^2 is directly related to the dissipation rate when, in a time-averaged sense, isotropic turbulence is uniformly advected downstream. Simonich and Bradshaw used Eq. (7) to calculate free-stream length scales downstream of a grid. Numerous authors (Table 1) have since used Eq. (7) to calculate free-stream length scales in decaying flows.

Our final scale for review was given by Ames and Moffat [12],

$$L_{II} = 1.5u'^3/\epsilon. \quad (8)$$

To estimate ϵ, Ames and Moffat fit the inertial subrange of a measured energy spectrum to the equation

$$E_1\{k_1\} = \frac{18}{55} A \epsilon^{2/3} k_1^{-5/3}. \quad (9)$$

Equation (9) results if the three-dimensional energy spectrum is modeled with a power-law relationship in the inertial subrange [2]. Ames and Moffat used a value of 1.62 for the constant A.

Summary of Merits and Deficiencies in Existing Scale Definitions

This summary is not an exhaustive discussion of the benefits or detriments of using the scales listed. This comparison highlights some general attributes of the conceptual and practical implications of using each scale. Attributes of the scales are summarized in Table 2. A merit common to these five scales is that they are all calculated using the streamwise fluctuating velocity, u': the fluctuating component most easily measured in many experiments.

A More Robust Energy Scale

An author may find a certain calculation method advantageous for experiment-specific reasons. However, to simplify the process of comparing results from different heat transfer investigations, a general consensus on a standardized calculation method would be useful. With a standardized method, in addition to any other length scales presented, authors could include the standardized scale values to reduce data comparison ambiguity.

When selecting a standard calculation method, we search for the following traits: versatility (ease of use in a number of different flows), historical concordance (results that are comparable with previously reported data), and clarity (process definition with enough detail to provide repeatability between investigators). With these criteria in mind, of the five scales reviewed, L_{II} holds the most promise as a standardized scale for the following reasons:

- the calculation requires information from only a single point in the flow field
- conceptually, the scale may be used in flows with mean velocity gradients if specific concerns related to Taylor's hypothesis are addressed
- the L_{II} scale is directly comparable with L_I which is widely used in the heat transfer literature

Table 2 Summary of merits and deficiencies of five length scale calculation methods

Scale	Merits	Deficiencies
Λ_I	Directly calculable from the autocorrelation curve. Does not rely on assumptions leading to a universal spectral curve. Directly relatable to dissipation of turbulent kinetic energy using isotropic assumptions and relationship between autocorrelation and spectrum.	Termination of integration can yield incorrect values; different flows can generate differently behaving and meaningful negative tails on the autocorrelation curve.
Λ_{II}	Simplicity of calculation. At large Reynolds numbers, results usually compare well with Λ_I values.	No rigorous/standardized "best fit" criteria; variation introduced between investigators. Up to +/-20% variation can still yield visually pleasing curve fits for moderate turbulence Reynolds numbers. Well-defined inertial subrange needed in measured spectrum to provide fitting capability over a wide range of wave numbers.
Λ_{III}	Simplicity of calculation.	Relies heavily on accurate extrapolation of low wave number portion of the measured spectrum. Low wave number range most sensitive to anisotropic effects. Also, because high sample rates are needed to obtain unaliased spectra and convergence of the low wave number range requires long sample times, large data file requirements accompany the proper use of this calculation method. (Of course, appropriate filtering techniques can reduce the file size requirements.)
L_I	Spectral information not required. Isotropic decay correlations may be used to verify downstream flow behavior. Easily related to dissipation of turbulent kinetic energy.	This scale cannot be used in any part of the flow where a production component is present (i.e., it cannot be used if a mean velocity gradient exists; this precludes its use within the boundary layer). It also cannot be calculated with information from only a single point in the flow field. Different techniques used to estimate the "measured" decay rate yield significantly different results.
L_{II}	Direct relationship to the dissipation of turbulent kinetic energy. Does not require information from multiple points in the flow field. Potential for use in flow field with mean velocity gradient. Equivalence with L_I for large Reynolds number flows in which L_I can be calculated.	No rigorous/standardized "best fit" criteria; variation introduced between investigators. Curve fit requires well-defined inertial subrange (large Re_t). While this scale may be useful in flows with a mean gradient, differences in local convection velocities that lead to spatial aliasing have not previously been addressed in the heat transfer literature.

In the remainder of this paper, we introduce and discuss a more robust energy scale calculation method that is based on L_{II}. The method is rigorously defined, lowers the turbulent Reynolds number at which the scale is calculable, and imposes limits that enable the scale to be confidently determined for flows with mean velocity gradients. While our scale is conceptually the same as L_{II}, to distinguish it from the other calculation methods, we call the scale L_e.

Background. From Tennekes and Lumley [1] we have, for isotropic turbulence,

$$\epsilon = \int_0^\infty D\{k_1\} dk_1, \tag{10}$$

where the dissipation spectrum is given by

$$D\{k_1\} = 2\nu k_1^2 E\{k_1\}. \tag{11}$$

Hinze [2] relates the three-dimensional energy spectrum to the one-dimensional spectrum,

$$E\{k_1\} = \frac{1}{2} k_1^2 \frac{d^2 E_1\{k_1\}}{dk_1^2} - \frac{1}{2} k_1 \frac{dE_1\{k_1\}}{dk_1} \tag{12}$$

so that we can generate the familiar result,

$$\epsilon = 15\nu \int_0^\infty k_1^2 E_1\{k_1\} dk_1. \tag{13}$$

Addressing time spectra measured in shear flows, Lumley [13] argues that, despite the mean shear, the trend toward isotropy in the dissipation range (the wave number range where most of the dissipation occurs) is very strong. We suspect that an isotropic estimate of ϵ obtained by integrating a measured dissipation spectrum may yield good results even in flows with mean velocity gradients. Lumley distinguishes between $E_1\{k_1\}$ and $E_1\{k_1\}_m$ (the subscript "m" refers to the measured spectra) because of "space" versus "time" spectra issues (issues that are related to the validity of Taylor's hypothesis and are presented later). Lumley gives a correction scheme for the high-wave-number region of the measured spectra in terms of the local fluctuating velocities,

$$E_1\{k_1\}_m = E_1\{k_1\} + \frac{Tu^2}{2}\left[\left(k_1^2 \frac{d^2 E_1\{k_1\}}{dk_1^2} - 2E_1\{k_1\}\right) - 2\left(k_1 \frac{dE_1\{k_1\}}{dk_1} + E\{k_1\}\right)\left(\frac{(v'^2 + w'^2)}{u'^2} - 2\right)\right]. \tag{14}$$

We substitute the solution to Eq. (12) [2],

$$E_1\{k_1\} = \int_{k_1}^\infty \frac{E\{k\}}{k}\left[1 - \left(\frac{k_1}{k}\right)^2\right] dk \tag{15}$$

into Eq. (14) and twice invoke Leibniz's rule to write

$$E_1\{k_1\}_m = \left(1 - Tu^2\left[1 + \left(\frac{v'}{u'}\right)^2 + \left(\frac{w'}{u'}\right)^2 - 2\right]\right) E_1\{k_1\} + Tu^2 E\{k_1\} + 2Tu^2\left[\left(\frac{v'}{u'}\right)^2 + \left(\frac{w'}{u'}\right)^2 - 2.5\right] k_1^2 \int_{k_1}^\infty \frac{E\{k\}}{k^3} dk. \tag{16}$$

Equation (16) assumes that the convect*ed* field is isotropic, but allows for anisotropy of the convect*ing* field. When the convecting field is also isotropic, Eq. (16) reduces to

$$E_1\{k_1\}_m = (1 - Tu^2) E_1\{k_1\} + Tu^2 E\{k_1\} - Tu^2 k_1^2 \int_{k_1}^\infty \frac{E\{k\}}{k^3} dk \tag{17}$$

illustrating that the measured one-dimensional spectrum is dependent on the local turbulence intensity as well as the form of the three-dimensional spectrum.

With Eqs. (10), (11), (12), and (17), Lumley shows that, for the isotropic convecting field, the resulting adjustment for a measured dissipation rate is given by

$$\epsilon = \epsilon_m / (1 + 5Tu^2). \tag{18}$$

Using Eq. (16) in the same manner, we find that the correction for the more general anisotropic case is

$$\epsilon = \epsilon_m (1 + Tu^2[1 + 2(v'/u')^2 + 2(w'/u')^2])^{-1}. \tag{19}$$

With a theoretical model of $E\{k_1\}$, Eqs. (15) and (16) allow us to predict the measured spectrum, $E_1\{k_1\}_m$, for a specified value of the local intensity. In this work the theoretical spectrum chosen was that of Panchev and Kesich as reported by Hinze [2] (p. 241).

Lumley [13] also gives criteria that can be used to determine when the spectral correction is valid; the energy distribution, mean velocity, and mean velocity gradient will determine the wave number range over which the correction may be applied. The pertinent relationships are given as

1 $k_1 \gg 2\pi (dU/dy)/U$ (to address convection velocity nonuniformity)
2 $E_1\{k_1\} \gg (2\pi^2/3)[(dU/dy)^2/U^2] d^2 E_1\{k_1\}/dk_1^2$ (considering spectral broadening)
3 $E_1\{k_1\} \ll\ll U^2/k_1$ (to verify a frozen convected pattern)
4 $E_1\{k_1\} \gg\gg 4\pi^2 (dU/dy)^2/k_1^3$ (negligible anisotropy due to mean shear)

Lumley recommends that the inequalities, $\gg$, be interpreted as a factor of three difference. However, using Reynolds stress spectra to support his position, he argues that the tendency toward isotropy is so strong in the high wave number range that weakening criterion four to simply exceeding equality will likely be satisfactory. We therefore adopt $E_1\{k_1\} \geqslant 4\pi^2 (dU/dy)^2/k_1^3$ as our fourth criterion.

Calculation Method. We now present the calculation method for L_e. The steps are as follows:

1 Measure the one-dimensional spectrum, $E_1\{k_1\}_m$.
2 Calculate ϵ_m using Eq. (13), $\epsilon_m = 15\nu \int_0^\infty k_1^2 E_1\{k_1\}_m dk_1$.
3 Apply Lumley's correction to get ϵ, $\epsilon = \epsilon_m/(1 + 5Tu^2)$ (isotropic case illustrated).
4 Check the agreement between the measured spectrum and the theoretical measured spectrum based on the corrected ϵ.
5 Check the validity of the correction for $k_1\eta > 0.05$ using Lumley's four criteria (η is the Kolmogorov length scale, $(\nu^3/\epsilon)^{1/4}$).
6 If the corrected ϵ is valid based on the checks in steps four and five, calculate L_e using the inviscid decay relation

$$L_e = \frac{3}{2}(u'^2)^{3/2}/\epsilon. \tag{20}$$

An Additional Consideration. There is an additional practical consideration that refines the calculation technique and fosters consistency between investigators. As the measured spectrum will have finite bandwidth, the upper and lower limits of the numerical integration in step two above must be values other than infinity and zero. In practice, for an adequately sampled velocity signal that has been low-pass filtered (i.e., the low wave number attenuation is due only to natural roll-off), substituting the lowest measured wave number for the lower limit is generally acceptable; the excluded portion of the spectrum contributes very little to the overall summation. The upper end of the measured spectrum, however, is highly dependent on sensor response (a function of wire size in hot-wire anemometry), filter cut-off frequency, and signal-to-noise ratio. For this reason it is recommended that the

integration be separated into two integrals. Starting at the lowest measured wave number, the first integral is terminated at a value of $0.2<k_1\eta<1.0$ where the actual and theoretical measured spectra agree to within 10 percent. Adequate sample-rate and sensor response characteristics will be required to meet this agreement constraint. The second integral then uses the theoretical measured spectra to carry the summation out to an upper limit of $k_1\eta=4$. The high-end roll-off of the dissipation spectrum makes integration beyond this value unnecessary.

Admittedly, this consideration increases the complexity of calculating ϵ by introducing an iterative component. However, based on the behavior observed during validation tests of the method, the improvement in sensitivity and consistency merits the added effort. From multiple-record samples of different stationary flows, experimental uncertainty in L_e was determined to be approximately 10 percent.

Advantages and Disadvantages of Using L_e. The new scale possesses the same advantages as L_{II} and overcomes the L_{II} disadvantages in Table 2. The integration method avoids "best fit" uncertainties and allows the calculation to be made at low Reynolds numbers. The low Reynolds number capability of L_e is a significant advantage. With the incorporation of Lumley's results, the scale can be calculated using the valid region of the spectrum despite the presence of a mean velocity gradient. This is a particularly attractive feature because it makes it possible to calculate the scale within a shear layer or boundary layer.

The primary disadvantage of L_e is the need to resolve a significant portion of the dissipation range. At large Reynolds numbers, this requires fast sample rates and very responsive sensors. Under these conditions the investigator may wish to use L_{II} instead. Fortunately, at high Reynolds numbers, there should be a well-defined inertial subrange and L_{II}, combined with Lumley's criteria, may yield useable results. However, by Lumley's criteria a large velocity gradient will invalidate the inertial subrange of the measured spectrum before the dissipation range; thus, the use of L_e may still be necessary.

Experimental Results. Figure 1 shows a measured energy spectrum to illustrate some of the previously addressed calculation issues presented in terms of the dimensional amplitude and nondimensional wave number. The spectrum shown meets all criteria for the range $0.04<k_1\eta<0.7$. The dissipation spectrum for the energy spectrum of Fig. 1 is presented in Fig. 2 to highlight the dissipation range. The high wave number range of dissipation spectra with attenuation due to filter response and elevation due to noise are shown in Fig. 3. In these cases the technique of splitting the integration to obtain ϵ is seen to yield good scaling in the range $0.05<k_1\eta<0.4$ for the attenuated signal and up to $k_1\eta=0.7$ for the noisy signal. This indicates that the integration was unaffected by the altered portion of the spectra and suitable ϵ values were obtained for these flows.

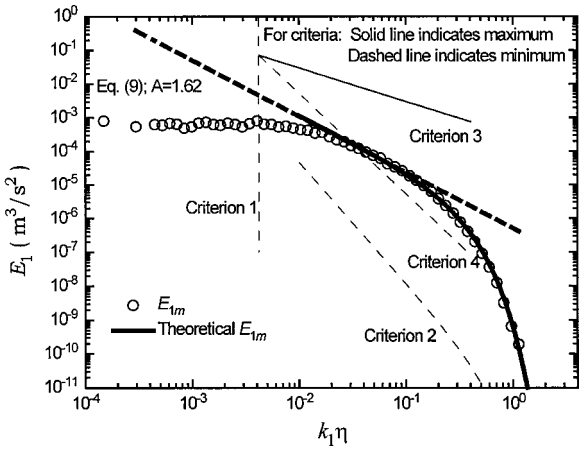

Fig. 1 Typical measured spectra with criteria and theory

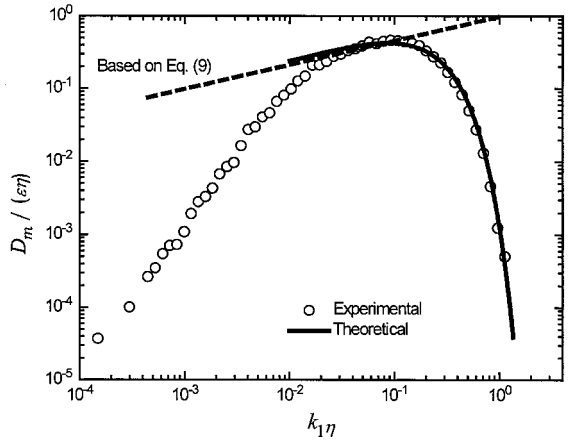

Fig. 2 Experimental and theoretical dissipation spectra

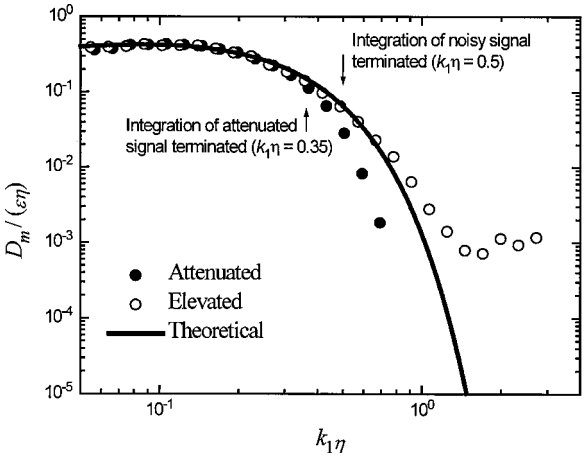

Fig. 3 High-end response characteristics

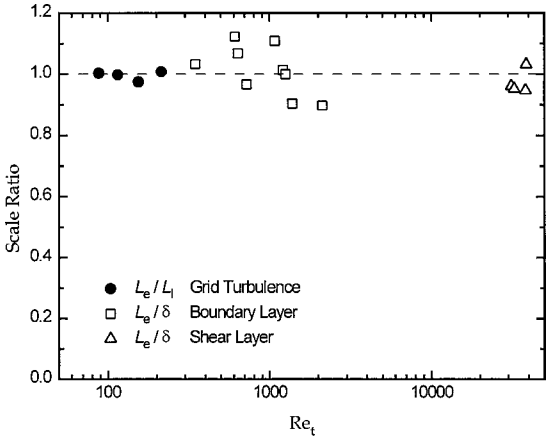

Fig. 4 Behavior of L_e in different types of flows

The L_e calculation method was tested in decaying grid-generated turbulence, near the center of a two-stream turbulent shear layer, and in the core of a turbulent boundary layer (without free-stream turbulence). Figure 4 shows the behavior of the calculation method for these three flows. The results show that the

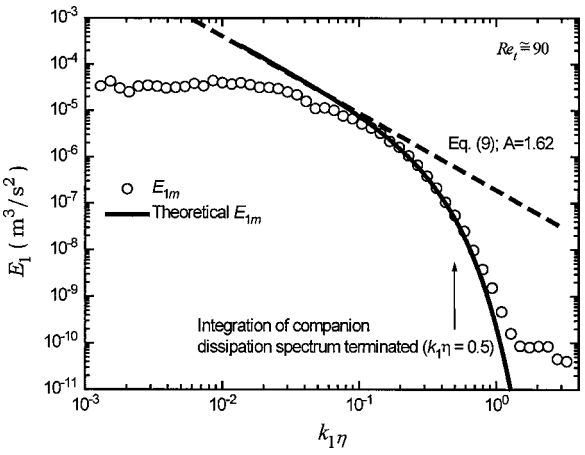

Fig. 5 Very low turbulent Reynolds number spectrum

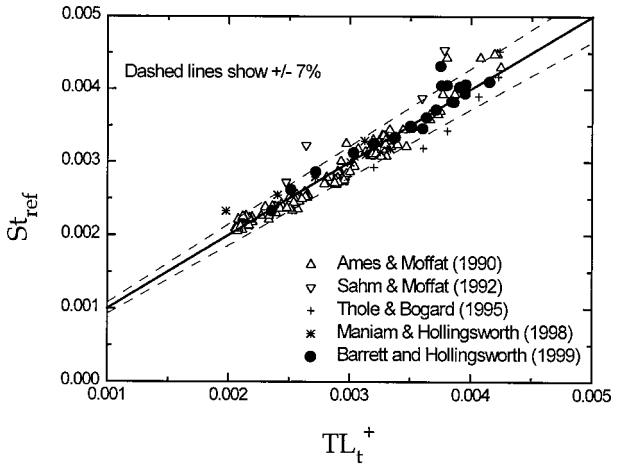

Fig. 7 Use of L_e in Stanton number correlation of Barrett and Hollingsworth [15]

ratio L_e/L_I downstream of a grid is unity as isotropic theory predicts. Examining the turbulent shear and boundary layers, the ratio L_e/δ, where δ is the vorticity thickness for the shear layer or the 99 percent thickness (based on free-stream velocity) for the boundary layer, is approximately one. This result reflects the accepted behavior of an integral scale as noted earlier. Figure 5 shows a very low turbulent Reynolds number spectrum ($Re_t \cong 90$) from the grid-generated turbulence case. The turbulent Reynolds number is given by $Re_t=[1.5(u')^2]^2/(\nu\epsilon)$. No inertial subrange is evident in Fig. 5, yet the L_e calculation matched the L_I calculation very well. Note that for this spectrum, L_{II} cannot be accurately determined.

The behavior of L_e across a turbulent boundary layer is shown in Fig. 6. The experimental values for $\nu\epsilon/u_\tau^4$ (using corrected, isotropic ϵ values) are compared with the DNS values calculated by Spalart [14]. The filled symbols denote points where all but the fourth of Lumley's criteria were satisfied; the open symbols represent points where the velocity gradient caused at least one of the other three criteria to be violated. In general, criterion four tends to be the most difficult to satisfy. But, as Lumley also noted, good results can be obtained assuming small-scale isotropy even when criterion four is not met. The point of departure from Spalart's curve is coincident with the violation of the remaining criteria and suggests that the criteria might be useful in dissipation calculations for other types of flows.

Finally, to explore the application of L_e in a heat transfer correlation, Fig. 7 presents results from Barrett and Hollingsworth [15] that indicate that the L_e scale is an appropriate choice to correlate a Stanton number based on a boundary-layer core reference temperature, $St_{ref} \equiv q_w/[\rho c_p(\overline{t_w}-\overline{t_{L_e^+}})U_\infty]$. The term $\overline{t_{L_e^+}}$ represents the mean temperature at a distance L_e from the wall. The parameter TL^+, developed in detail in the referenced work, is an involved expression that incorporates the L_e length scale described herein.

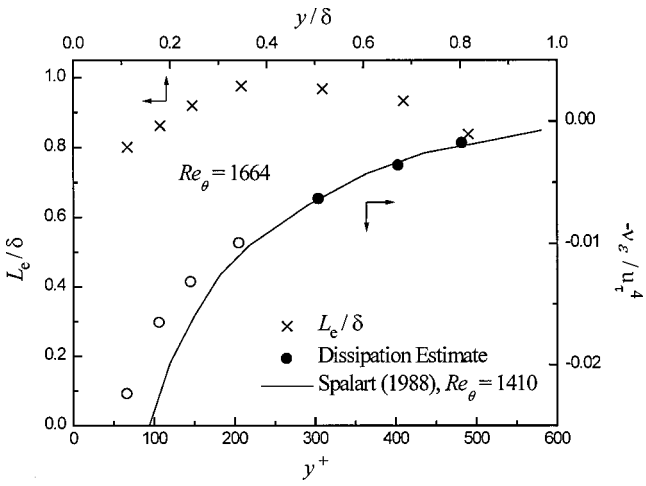

Fig. 6 Boundary layer scale and dissipation evaluation

Conclusions

To improve the comparability of heat transfer data between experimenters, a detailed method of calculating a turbulent length scale will be helpful. The authors recommend that L_e be adopted as a standard for the following reasons:

1 The method uses measurements from only a single-point in the flow field.
2 The method can be employed in flows with mean velocity gradients.
3 A well-defined inertial subrange is not required in the energy spectrum; the scale is calculable in low turbulent Reynolds number flows.
4 The scale is equivalent to L_I and L_{II} in flows in which the latter scales can be determined.
5 The scale can be calculated from the same information used to calculate Λ_I (a Fourier transform of the autocorrelation curve produces the energy spectrum); the added computation relative to Λ_I is minimal.
6 The method includes criteria to determine when the technique is invalid.
7 The calculation is more rigorous than "best fit" methods.

Acknowledgments

The authors would like to thank Dr. S. J. Kleis for the use of his wind tunnel facility and for his continuing interest and involvement. We also thank Dr. B. M. Maniam for providing the data for the two-stream mixing layer test case. These experiments have been supported by the Texas Higher Education Coordinating Board Advanced Technology Program through Grant # 003652-944, the UH Institute for Space Systems Operations, and the UH Energy Laboratory. Dr. Barrett received additional support from the NASA/Texas Space Grant Consortium and the SAE Doctoral Scholars Program.

Nomenclature

A = constant used in power-law fit of energy spectrum
D = dissipation spectrum

E = power spectral density of fluctuating velocity
L = experimentally determined length scale related to ϵ
R_{11} = Eulerian autocorrelation coefficient
Re_θ = momentum-thickness Reynolds number ($=U_\infty\theta/\nu$)
Re_t = turbulent Reynolds number ($=(1.5(u')^2)^2/(\nu\epsilon)$)
T_{11} = Eulerian integral time scale [defined in the text]
Tu = turbulence intensity ($=u'/U$)
U = time-mean Eulerian velocity in principal flow direction
c_p = specific heat
f = frequency
k = wave number
$\underline{q}$ = heat flux
t = mean temperature
u' = RMS fluctuating velocity in principal flow direction
u_τ = boundary layer friction velocity ($=\sqrt{\tau_w/\rho}$)
v', w' = RMS fluctuating velocities in non-principal flow directions
x = streamwise distance
y = distance from wall
y^+ = dimensionless distance from wall ($=yu_\tau/\nu$)
Λ = experimentally determined length scale related to Λ_f
Λ_f = Eulerian integral length scale (defined in the text)
δ = shear-layer vorticity thickness or boundary-layer thickness
ϵ = dissipation of turbulent kinetic energy
η = Kolmogorov length scale ($=(\nu^3/\epsilon)^{1/4}$)
θ = momentum thickness of the boundary layer
ν = kinematic viscosity
ρ = density
τ = shear stress

Subscripts

1 = x-component related
∞ = free-stream
$I-III$ = scale tracking reference
e = energy-based
m = measured
t = turbulent
w = value at the wall in a wall-bounded flow
θ = based on momentum thickness

References

[1] Tennekes, H., and Lumley, J. L., 1972, *A First Course in Turbulence*, MIT Press, Cambridge, MA.
[2] Hinze, J. O., 1975, *Turbulence*, McGraw-Hill, New York.
[3] Young, C. D., Han, J. C., Huang, Y., and Rivir, R. B., 1992, "Influence of Jet-grid Turbulence on Flat Plate Turbulent Boundary Layer Flow and Heat Transfer," ASME J. Heat Transfer, **114**, pp. 65–72.
[4] Van Fossen, G. J., Simoneau, R. J., and Ching, C. Y., 1995, "Influence of Turbulence Parameters, Reynolds Number, and Body Shape on Stagnation-region Heat Transfer," ASME J. Heat Transfer, **117**, pp. 597–603.
[5] Camp, T. R., and Shin, H.-W., 1995, "Turbulence Intensity and Length Scale Measurements in Multistage Compressors," ASME J. Turbomach., **117**, pp. 38–46.
[6] Moss, R. W., and Oldfield, M. L. G., 1996, "Effect of Free-Stream Turbulence on Flat-plate Heat Flux Signals: Spectra and Eddy Transport Velocities," ASME J. Turbomach., **118**, pp. 461–467.
[7] Hollingsworth, D. K., and Bourgogne, H.-A., 1995, "The Development of a Turbulent Boundary Layer in High Free-stream Turbulence Produced by a Two-stream Mixing Layer," Exp. Therm. Fluid Sci., **11**, pp. 210–222.
[8] Maniam, B. M., and Hollingsworth, D. K., 1998, "Experimental Investigation of Heat Transfer in a Three-Dimensional Boundary Layer Beneath a Mixing Layer," *Proceedings, 7th AIAA/ASME Joint Thermophysics and Heat Transfer Conference*, Paper 12-HT-3.1, Albuquerque, NM, June 15–18.
[9] Thole, K. A., Bogard, D. G., and Whan-Tong, J. L., 1994, "Generating High Freestream Turbulence Levels," Experiments in Fluids, **17**, pp. 375–380.
[10] Johnson, P. L., and Johnston, J. P., 1989, "The Effects of Grid-Generated Turbulence on Flat and Concave Turbulent Boundary Layers," Report No. MD-53, Department of Mechanical Engineering, Stanford University, Stanford, CA.
[11] Simonich, J. C., and Bradshaw, P., 1978, "Effect of Free-Stream Turbulence on Heat Transfer through a Turbulent Boundary Layer," ASME J. Heat Transfer, **100**, pp. 671–677.
[12] Ames, F. E., and Moffat, R. J., 1990, "Heat Transfer with High Intensity, Large Scale Turbulence: The Flat Plate Turbulent Boundary Layer and the Cylindrical Stagnation Point," Report No. HMT-44, Department of Mechanical Engineering, Stanford University, Stanford, CA.
[13] Lumley, J. L., 1965, "Interpretation of Time Spectra Measured in High-intensity Shear Flows," Phys. Fluids, **8**, pp. 1056–1062.
[14] Spalart, P. R., 1988, "Direct Simulation of a Turbulent Boundary Layer up to $R_\theta=1410$," J. Fluid Mech., **187**, pp. 61–98.
[15] Barrett, M. J., and Hollingsworth, D. K., 1999, "On the Correlation of Heat Transfer in Turbulent Boundary Layers Subjected to Free-stream Turbulence," *Proceedings of the 33rd National Heat Transfer Conference*, ASME Paper HTD99-76; Albuquerque, NM, August 15–17.
[16] Blair, M. F., 1983, "Influence of Free-stream Turbulence on Turbulent Boundary Layer Heat Transfer and Mean Profile Development: Part II—Analysis of Results," ASME J. Heat Transfer, **105**, pp. 41–47.
[17] Hancock, P. E., and Bradshaw, P., 1989, "Turbulence Structure of a Boundary Layer Beneath a Turbulent Free Stream," J. Fluid Mech., **205**, pp. 45–76.
[18] Castro, I. P., 1984, "Effect of Free Stream Turbulence on Low Reynolds Number Boundary Layers," ASME J. Fluids Eng., **106**, pp. 298–306.
[19] Hancock, P. E., and Bradshaw, P., 1983, "The Effect of Free-stream Turbulence on Turbulent Boundary Layers," ASME J. Fluids Eng., **105**, pp. 284–289.
[20] Sahm, M. K., and Moffat, R. J., 1992, "Turbulent Boundary Layers with High Turbulence: Experimental Heat Transfer and Structure on Flat and Convex Walls," Report No. HMT-45, Department of Mechanical Engineering, Stanford University, Stanford, CA.
[21] Ames, F. E., and Plesniak, M. W., 1995, "The Influence of Large Scale, High Intensity Turbulence on Vane Aerodynamic Losses, Wake Growth, and the Exit Turbulence Parameters," *Proceedings, International Gas Turbine and Aeroengine Congress and Exposition*, ASME Paper 95-GT-290, Houston, TX, June 5–8.
[22] Thole, K. A., and Bogard, D. G., 1995, "Enhanced Heat Transfer and Shear Stress Due to High Free-Stream Turbulence," ASME J. Turbomach., **117**, pp. 418–424.
[23] Thole, K. A., and Bogard, D. G., 1996, "High Freestream Turbulence Effects on Turbulent Boundary Layers," ASME J. Fluids Eng., **118**, pp. 276–284.
[24] Ames, F. E., 1997, "The Influence of Large-Scale High-Intensity Turbulence on Vane Heat Transfer," ASME J. Turbomach., **119**, pp. 23–30.
[25] Bott, D. M., and Bradshaw, P., 1998, "Effect of High Free-Stream Turbulence on Boundary Layer Skin Friction and Heat Transfer," *Proceedings, 36th Aerospace Sciences Meeting & Exhibit*, Reno, NV, AIAA Paper 98-0531, January 12–15.